J. Condensed Matter Nucl. Sci. 8 (2012) 75–90

Research Article

Model for Electromagnetic pulsed BEC Experiments

Roger S. Stringham *

First Gate Energies, PO Box 1230 Kilauea, HI 96754, USA

Abstract

Sonofusion experiments, which incorporate transient Bose Einstein condensates, BEC, have recently focused on related sono-superconductivity. Cavitation jets implant high-density deuteron clusters into a target foil. Clusters are then squeezed by accelerated charges that form dense transient EM pulses. Cavitation and the associated sonoluminescence phenomena, used as a measuring tool, helps develop and explain related experimental results. Two outcomes, sonofusion and sono-superconductivity both produce D^+ clusters in reactors of different geometries. MHz reactor No. 1 is driven by a disk piezo and has produced excess heat, Q_x, using the foil target and other products, including ^{4}He. The new MHz reactor No. 2 is driven by a cylindrical piezo low power with a concentric wire target with transient cluster steady state concentration near the wire surface. The target's steady state cluster coverage may satisfy a sono-superconductivity subsurface cluster connectivity during the MHz's 100 ns collective sonoluminescence pulse. It was anticipated that ambient sono-superconductivity was possible but so far has proved difficult to measure. Cavitation D_2O bubbles in both reactors were controlled by three main parameters for the two reactors: temperature, pressure of Ar gas over D_2O, and acoustic watt input; T_i, P_i, and Q_a. The z-pinch jets' contents of deuterons and electrons were implanted, with an induced picosecond transient charge separation. This charge separation produced an electromagnetic, EM, cluster compression pulse that formed a high-density BEC environment, as the EM pulse pressure overwhelmed repulsive deuteron cluster pressure for that picosecond. This model used unique attributes of the high-density transient deuterons to produce sonofusion in reactor No. 1 and sono-superconductivity in reactor No. 2 near ambient temperature. The measurements showed the presence of sonoluminescence pulses, implanted plasma, and heat pulse ejecta sites.
 ISSN 2227-3123

Keywords: BEC, Deuteron, Sonoluminescense, Superconductivity, z-pinch

1. Introduction

The presented model can explain experimental results of 23 years of cavitation and sonoluminescence investigation of sonofusion. Cavitation piezo frequencies ranged from 20 kHz to 2.5 MHz, and showed definite advantages at the higher frequencies. The naturally selected cavitation resonant bubbles produced by a MHz feedback oscillator were very small 0.2 μm for the initial radius, R_i. The resonance control parameters of circulating D_2O were temperature, T_i, the pressure of Ar over the D_2O, P_i, and acoustic watt input, Q_a or Ap. These were all adjusted experimental

*E-mail: firstgate@earthlink.net; Tel.: 808 826 7530

 ISSN 2227-3123

conditions [1]. The small selected bubbles starting with a radius R_i of 0.2 μm, expanded isothermally to a maximum radius of 2.0 μm, R_o (see Fig. 1). This was followed by a sub-microsecond adiabatic collapse in the positive pressure zone of the acoustic wave to the final radius of 0.02 νm, R_f, about a 0.1 νs inertial compression process. This bubble is transient cavitation bubble that produces a high-energy density terminal bubble, radius R_f. The internal kinetic energy density of the transient cavitation bubble is KE/m^3 = $10^{-11}/R_f^3$ in J/m^3. Sonoluminescence pulses in reactor No. 1 with an acoustic input, Q_a, of 2 W was not detected, while in reactor No. 2, an acoustic watt input, Ap, of 2 W was near saturation. The MHz devices, with reactor volumes 0.3–1 cm^3, a reactor mass of 20–50 g, and mass flow rate of D_2O of 0.55 cm^3/s produced the same excess heat, Q_x, as the 46 and 20 kHz systems and were 1000 times larger [x]. High frequencies also produced a more intense sonoluminescence pulse, which was used to monitor the sonofusion process and its partial dense plasma. Cavitation systems followed a natural process, and with some control of parameters, T_i, P_i, and Q_a, were guided to produce usable power. During the bubble selection process only a fraction of the bubbles had the R_i that would couple to the frequency of the piezo resonator. The rest of the bubbles within the piezo influence had little involvement with the sonofusion process. (*Note*: The transient cavitation bubble in the model existed for one acoustic cycle.) Sonoluminescence was used as a tool to gauge the relative number of deuterons in the high density excited state in the bubble's final radius, R_f, of the pseudo adiabatic collapse (Fig. 2). The collapsing bubble produced at the same moment, the sonoluminescence pulse (Multi Pixel Photon Counting, MPPC), and a high-density z-pinched plasma jet with its contents squeezed by the EM pressure and implanted into a nearby target at a velocity of about 30 km/s [2–4].

2. General Set-up for Reactor Nos. 1 and 2

It was necessary for the SL pulse measurements that monitored the MHz piezo operation to be made in a black felt lined light box cooled by a small fan circulating outside air that removed heat from the box [5] (see Fig. 3). Calorimetry could be performed on reactors using the flow through type of calorimeter. A Measurement Computing USB 1608 HS collected data from an Ohio Semiconductor PC5 103CX5 that measured the total watts in, Q_i, and several type K thermocouples measured temperatures. A pressure device measured Ar pressure over the D_2O. A variac controlled the

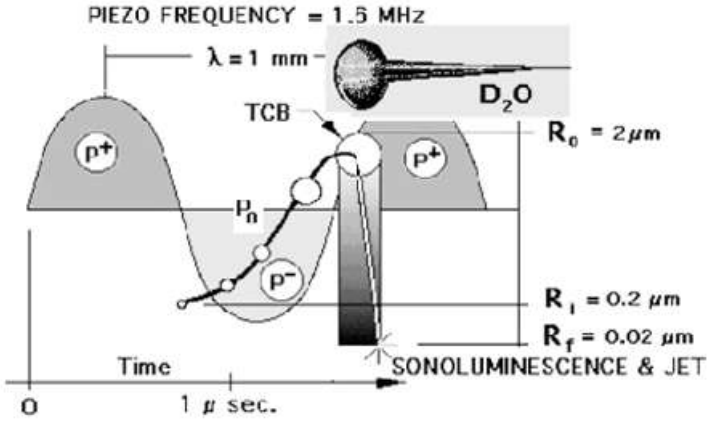

Figure 1. The 1.6 MHz TCB cycle .

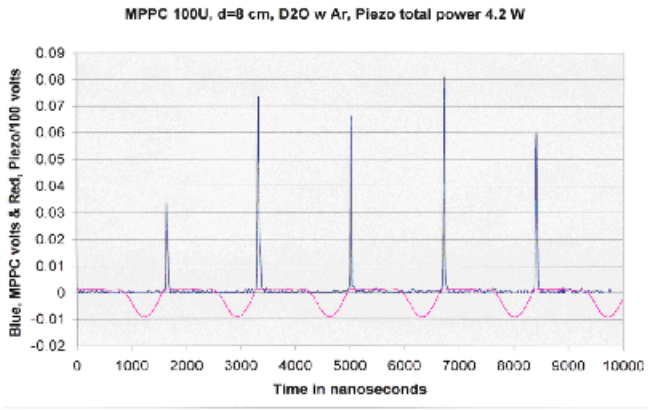

Figure 2. The MPPC SL pulse and MHz piezo volts.

power to the transformer that was measured by a watt meter and powered a feedback oscillator that drove the MHz piezo with the acoustic watt input, Q_a , of reactor No. 1 or Ap of reactor No. 2 [4]. The D_2O circulation loop of the reactors connected components with 1 mm inside diameter tubing. D_2O was circulated by an FMI metering pump, model QV, into a circular tubing heat exchanger, then a 10 μm particle filter at a flow rate of 0.55 cm^3/s At the reactor ports DT, T_{in} - Tout, and the flow of D_2O was measured through the reactor volume. The flow progressed to a flow meter and a bubbler where Ar gas pressure was monitored, and then back to the pump completing the calorimetry of the D_2O cycle (Figs. 3 and 4). Temperatures, pressures, power, and flow rates were collected from the reactors for processing. The 50 W, 120 V at 60 cycles variable power supply powered a feedback type oscillator that sensed any change in reactor temperature, and amplified that signal as the acoustic watt input, Q_a or A_p, at its resonance frequency. Q_a and Ap MHz signals were pulsed at 120 cycles/s, an envelope for the MHz signal. Reactor No. 2 used the same set-up (Figs. 3 and 4).

3. General Calorimetry

Calorimetry was a flow through type calorimetric measurement of $\Delta T = T_{out} - T_{in}$ with several thermocouples. Equally important was the D_2O flow per second measurement of mass flow, MF. DT*MF*4.669 equals the measured output watts, Q_o; this was the basic calorimetry. 4.669 was a scaling factor for converting heated D_2O from calories to joules. $Q_o - Q_a = Q_x$ [2]. The acoustic input, Q_a , was 0–16 W. A wattmeter measured Q_i and an efficiency factor of 0.30 converted Q_i to Q_a , $0.3Q_i = Q_a$. The amount of Q_x measured was the difference between the measured total heat out, Q_o, minus Q_a the acoustic watts input. The relationship between these three, sonoluminescence, Q_i, and Q_x, were plotted (Fig. 5).

4. General ^{4}He Measurement

The circulation of D_2O through the reactor provided easy access to the ejecta that included the fusion products heat and ^{4}He. The ^{4}He fusion product was circulated in the D_2O and could be collected at any time using standard gas expansion into evacuated gas sampling volumes for measurement. Helium four was measured from a stainless steel 50 cm^3 gas sample from circulating D_2O in the low frequency, 20 kHz, reactor. The gases were analyzed using the mass

spectroscopy facilities of the DOE's laboratory at the Rocketdyne Corp. in Southern California where Brian Oliver measured ^{4}He at 552 ppm at a $\sigma \pm 1$ ppm [6]. The 65 W of Q_x was measured by calorimetry over a 19 hour period.

5. Reactor No. 1 Set-up

The reactor was in a light box, and the DC electric input Q_i, powered the MHz oscillator and the piezo acoustic input, Q_a and the sonoluminescence photomultiplier, Hamamatsu ^{3}He 125, along with the Systron-Donner counter/timer that was used for measurements. The D_2O circulation system powered by an FMI pump in line with a filter circulated the D_2O at a constant rate to the reactor $T_{in} - T_{out} = \Delta T$. D_2O flow continued to the two liter H_2O bath and 2 mm $\times$ 3 m stainless steel cooling coil and through the flow meter to a bubbler and back to the pump. Reactor No. 1 used a larger acoustic input, Q_a, to the PZT piezo disk, 2 mm thick and 22 mm in diameter. Q_a was distributed over the disk's central 1/3 surface area while measuring excess heat production, Q_x. The disk was clamped at its periphery. The geometry was a 1 cm$^2 \times$ 100 μm thick target foil located 1 mm from the piezo surface, with circulating D_2O passing between the disk and the target. A small resistance heater placed in reactor No. 1's D_2O flow-through volume was used for calibration purposes. Figures 1 and 3 show the transient cavitation bubble evolution and time line that resulted in the SL pulse and z-pinch jet. The R_f bubble energy density produced by the pseudo adiabatic collapse launched the dense plasma jet at about 30 km/s accelerating to the target lattice. The photon pulses were made up of millions of individual sonoluminescence 100 ns bubble emissions, from each of the thousands of collapsing transient cavitation bubbles during 1 acoustic cycle, 10^{-6} s. z-Pinched deuterons and electrons of the jet plasma were implanted into a target

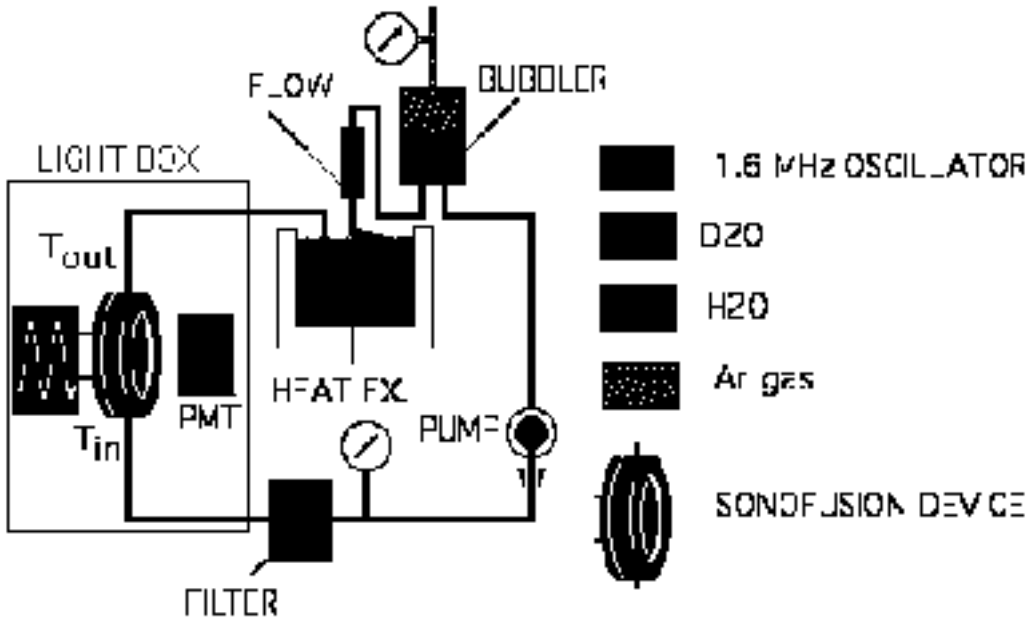

Figure 3. Reactor No. 1, sonofusion set-up.

Figure 4. Reactor No. 2 superconductivity set-up with MPPC.

producing a femto-second electron deuteron charge separation. Accelerated electrons compressed deuterons into BEC clusters via a picosecond EM pulse. An example of Q_x heat from DD fusion generation from reactor No. 1 is shown in Fig. 5. The picosecond time line for the compression pressures and evaporative deuteron cooling with the increasing repulsive escape pressure allowed for a low temperature and high density DD fusion event much like muon fusion (see Figs. 6 and 8). No ^{4}He measurements were made of gases in MHz reactors. The measurement of excess heat, Q_x, from calorimetric measurements, showed no measurable amount of radiation. Ejecta sites originating from fusion heat pulses were measured by SEM surveys of target foil surfaces showing their frequency differences and correlate to Q_x [2]. The low piezo frequencies, 20 and 46 kHz, had a broad size distribution and produced many multi-fusion events. MHz piezos had a 50 nm diameter ejecta site indicating a single fusion event per cluster of about 20 MeV in magnitude [2,7]. The sequence of producing and compressing deuteron BEC clusters also applies to reactor No. 2 systems.

6. Reactor No. 1, MHz Experiment

The 1.6 MHz experimental system produced the data shown in Fig. 5. The advantage to using the low-mass system was the time, about 60 s, for a 90% temperature response to its steady state temperature – heating and cooling curves. The D_2O residence circulation time was about 1 s in the 1 cm^3 reactor volume at a flow rate of 0.55 cm^3/s The external pressure, P_i, for these runs was 1–2 atm of argon. In the calibration mode the sonofusion device used a joule heater replacing Q_a , and $Q_x = 0$. To guard against radio-frequency interference, all DT measurements were made during the off mode of the piezo, no Q_a [4]. The heat capacity of reactor No. 1 was measured and surface convection was

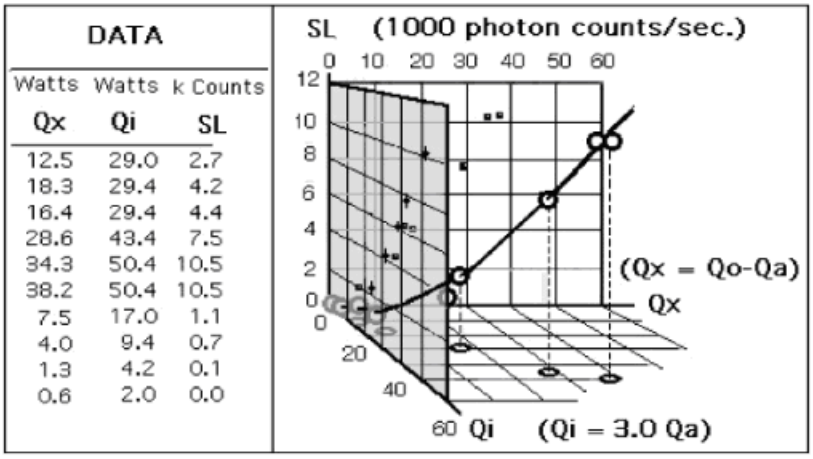

Figure 5. Reactor No. 1, sonofusion results of model BEC clusters.

estimated to be small at these low DTs. The calibration mode demonstrated the heat characteristics of reactor No. 1. At these flow rates about 90% of heat is removed by D_2O circulation. Figure 5 depicts one of many short experiments that showed Q_x where the input power, Q_i, was varied via a power variac into (low mass) reactor No. 1. The output power, Q_o, was measured as reactor No. 1 approached its steady state temperature [2,4,5].

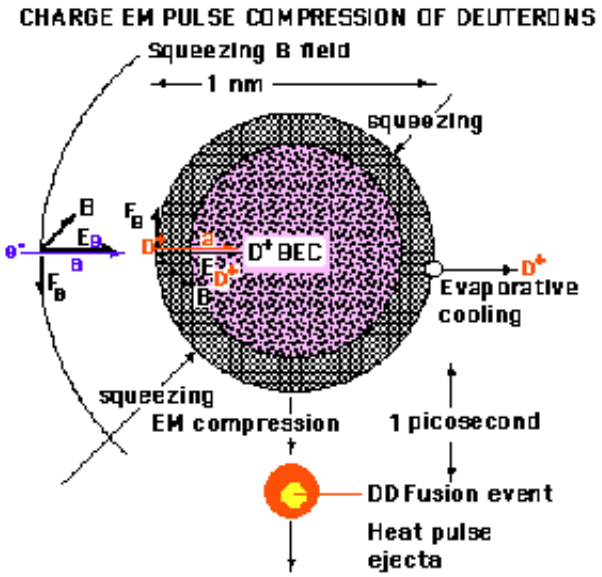

Figure 6. The cluster fusion of deuterons.

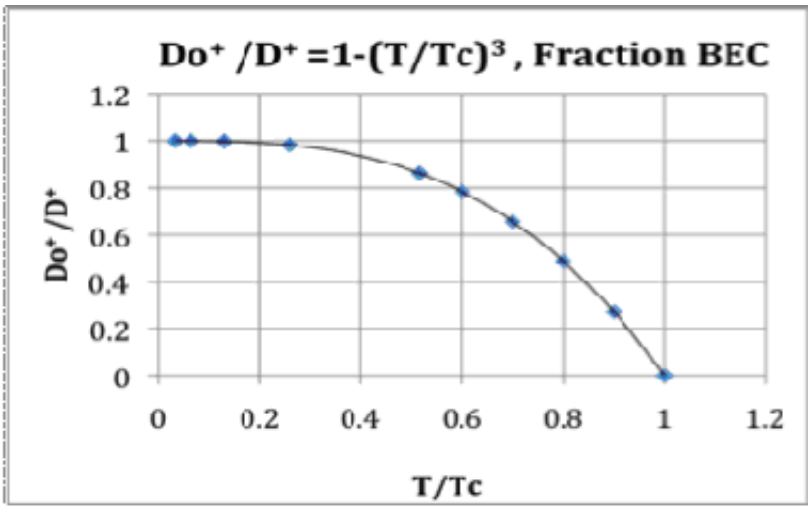

Figure 7. A smaller T/T_c drives cluster into a BEC.

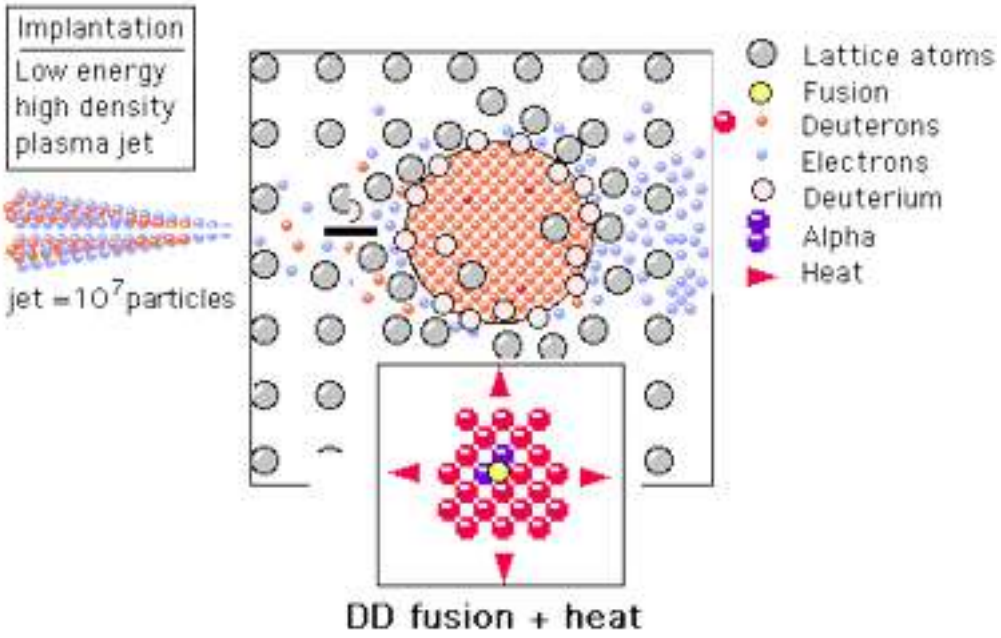

Figure 8. *Z*-Pinch jet implantation and BEC SF cluster.

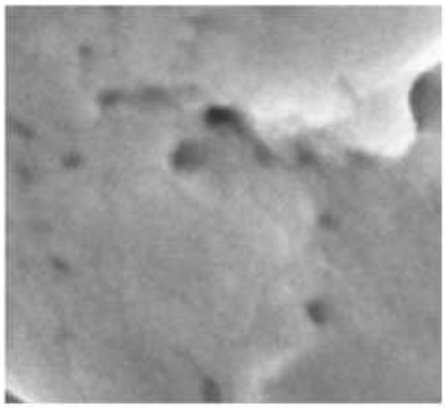

Figure 9. 100 μm thick Pd SEM 1 sq, μm at 46 kHz.

7. General Cluster

The following is directed towards sonofusion's Q_x, heat of fusion of $2D^+$ (Figs. 6–8). Immediately after the implant of the Coulombically squeezed z-pinch jet's dense plasma of electrons and deuterons into the lattice foil, the trapped deuterons attract the mobile electrons. The accelerating electrons compressed the deuterons with a collective EM pulse for a picosecond [3]. The 1 cm^2 and 100 μm thick Pd target lattice contained the compressing clusters, each with the potential characteristics of an inertial confined fusion system. The picosecond pulse pressures of EM compression were initially far greater than the constant escape pressure of Coulombic repulsion of the cluster deuterons. The BEC compressing environment of the cluster existed for that picosecond. These opposing pressures reversed their position after a picosecond and all the particles were dispersed, but in the case of reactor No. 1 DD fusion conditions were reached. Continuous evaporative cooling of the surface of escaping deuterons during this picosecond controlled the

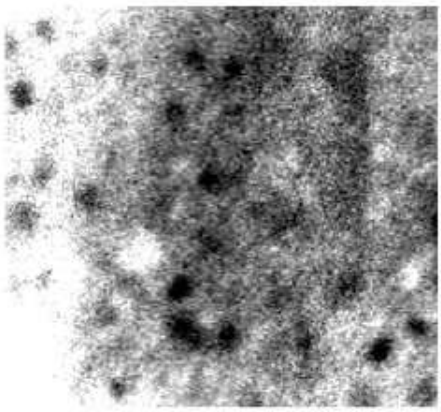

Figure 10. 100 μm thick Pd SEM 1 sq, μm at 1.6 MHz.

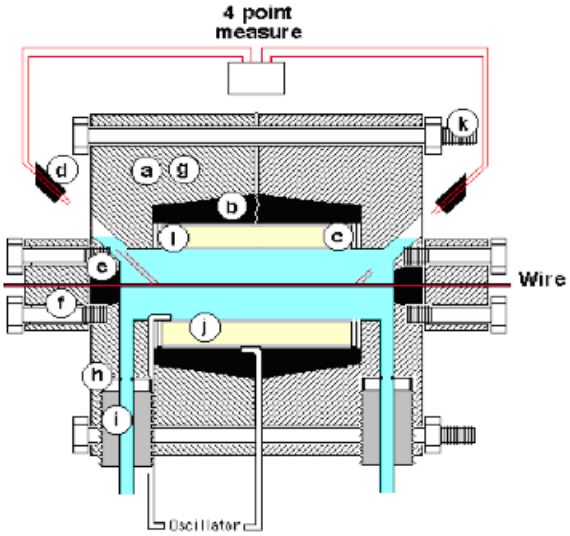

Figure 11. Reactor No. 2 – D_2O flow and piezo squeeze.

environment cooling the remaining cluster deuterons. Over this picosecond as many as one-half of the cluster deuterons evaporated as surface deuterons and removed heat from the BEC cluster. It was important for the BEC cluster's stability for it to remain as cool as possible as the cluster's energy density increased. The BEC cooling mechanism helped to maintain the unique properties of the BEC cluster. The deuterons are compressed to extreme densities by the EM pressure pulse focused on the cluster contents during the picosecond of electron acceleration. In low-frequency kHz systems both single and multiple DD fusion events occur in the cluster's BEC environment. Q_x heat pulse and ejecta sites in the 1 μm^2 area SEM survey photo are shown in Fig. 9. At a MHz, only single DD fusion events were found in the SEM Pd target foil photo (Fig. 10). The single events, 4×10^{-12} J/event, produced 50 nm ejecta sites in a μm^2 100 μm . SEM Figs. 9 and 10 are by Jane Wheeler, Evans Lab., Sunnyvale, CA. Figure 9 shows that the 46 kHz ejecta sites are fewer and have a much wider size distribution having multiple fusion events where the MHz system (Fig. 10) has more ejecta sites per μm^2, all about the same ejecta size [2].

The heat pulse generated by the DD fusion event approached, during a picosecond, densities of a white dwarf star and muon DD fusion. The heat of DD cluster fusion was distributed to the BEC's cluster deuteron population before a gamma could be formed. Then the heat from the cluster was passed on to the target lattice as a heat pulse. Ejecta vapor that included the fusion products and target lattice atoms from the expanding DD fusion heat pulse were ejected into the circulating D_2O where fusion products were collected and measured. One more important question on this path to DD fusion was the critical temperature, T_c, of the BEC cluster, and how it could be so high. The answer is the absence of electrons. The nuclear dissociation of a deuteron is 2.23 MeV. The deuteron has no accessible energy levels before its dissociation. The cluster is nuclear, not chemical and has none of the usual atom associated electrons. This difference is important. A BEC of atoms forms at ground state well below its next energy level, which is a small fraction of an eV. The neutron–proton boson is nuclear with no energy levels other than ground state. The cluster's high-density compression occurred in a collection of deuteron bosons with no electrons. There was a change of phase as the cluster density increased and the temperature decreased via D^+ evaporation. As D^+ bosons were compressed in the BEC, in the D_O^+ cluster, nearly all D^+ were in the condensed phase (Fig. 7). The deuteron cluster, free of electrons for a

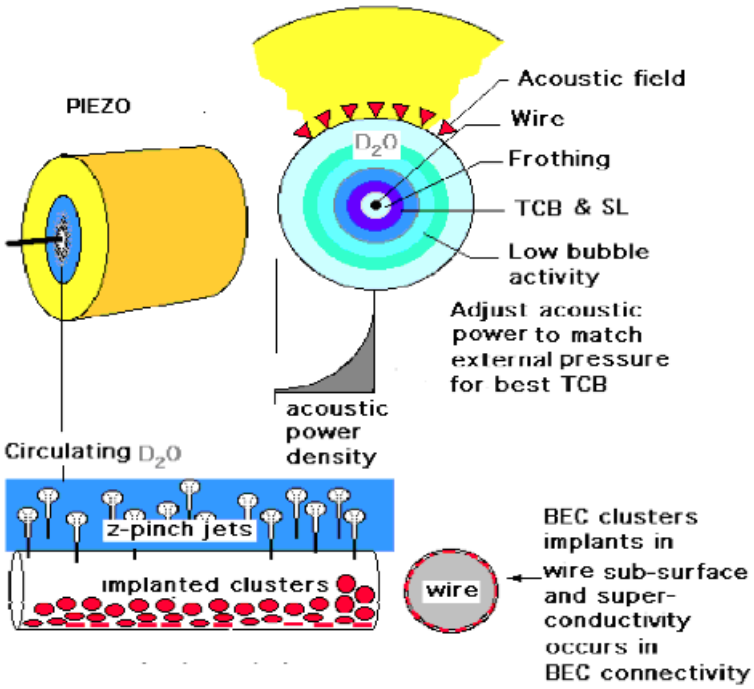

Figure 12. Reactor No. 2 – Piezo and target wire.

picosecond, had a particularly high critical temperature, T_c. The cluster temperature, T, of several eV was well below its nuclear T_c. The cluster D^+ population ratio, $D_O^+/D^+ = 1 - (T/T_c)^3$, changes with decreasing T. The compressing and cooling cluster's BEC phase moved the bulk of the cluster's deuterons into the BEC phase, D_o^+. Normally BECs, ultra cold boson atoms, not nuclei, have atomic energy levels at a small fraction of an MeV. Normally boson atoms

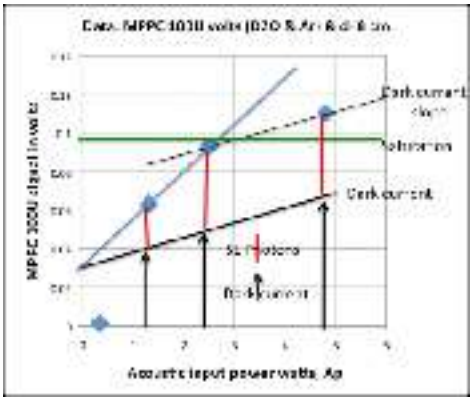

Figure 13. The MPPC photon measurement.

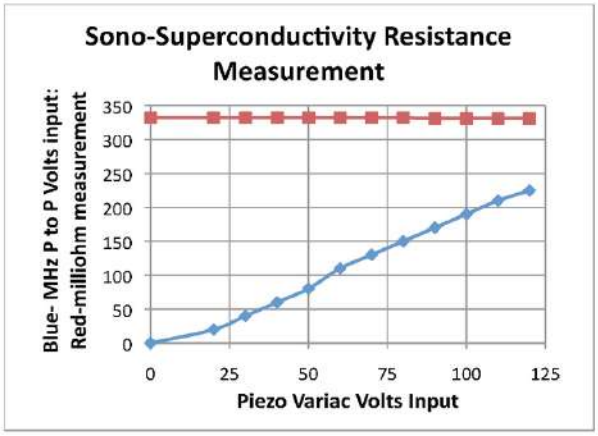

Figure 14. Reactor No. 2, superconductivity non-results.

must have low T_c temperatures and low pressure for their bosons to form a BEC phase based on their energy levels. The nuclear energy levels for light nuclei like the deuteron in the Shell and Collective models are large, MeV, compared to atomic energy levels of light boson atoms, a fraction of an eV. The BEC phase for the deuteron in the model was close to 100% when the cluster was at 4000 K (Fig. 7). The EM compression pulses easily met the conditions of a BEC cluster via the Shell Model. The picosecond time line for the compression pressures and evaporative deuteron cooling with the increasing repulsive escape pressure allowed for a low temperature and high-density DD fusion event much like muon fusion (see Figs. 6 and 8).

8. Reactor No. 2 and Set-up

The terms Q_a and Ap are equivalent for measurements of acoustic watt inputs driving piezos in reactors Nos. 1 and 2. The Ap of the cylindrical piezo converts its displacement to acoustic pressure wave that focuses at the center of the D_2O flow. Figure 12 shows the bubble collapse, z-pinch, implantation, and cluster compression. Reactor No. 2 depends on the increasing focused acoustic energy density at the wire surface. This allows for very small acoustic inputs Q_a in the order of 1 W to produce sonoluminescence. The objective is to implant a higher density of sub-surface BEC clusters that will network at a steady state concentration. New oscilloscope voltage measurements in this environment hopefully will show the model's superconductivity

Reactor No. 2 has its PZT piezo outer surface clamped with a surrounding hard rubber sheath while circulating D_2O at a rate of 0.55 cm^3/s through its 0.3 cm^3 volume. See clamping bolts (k) in Fig. 11. The target was a fine wire, 100 μm Pd, and the objective was finding an ambient temperature superconductivity path associated with the BEC cluster model. The Hamamatsu MPPC S10362-11- series of multi pixel photon counters with a DC power supply, HP 6034 A, was used to measure the sonoluminescence photons (Fig. 2). The driving piezo had a cylindrical geometry 1.7 mm in length, 12 mm OD, and 5 mm ID. The MPPC DC volt output signal was processed by an ORTEK VT120A preamp. This cylindrical piezo concentrated energy along its central axis. The sonoluminescence measurements in reactor No. 2 were difference measurements, piezo on – piezo off in the light box. The MPPC signal data was passed through the ORTEK preamp to the oscilloscope. The absolute value of this photon difference signal included the dark current, other interference, and counted photons (Figs. 2 and 13). The oscilloscope measured two channels of data.

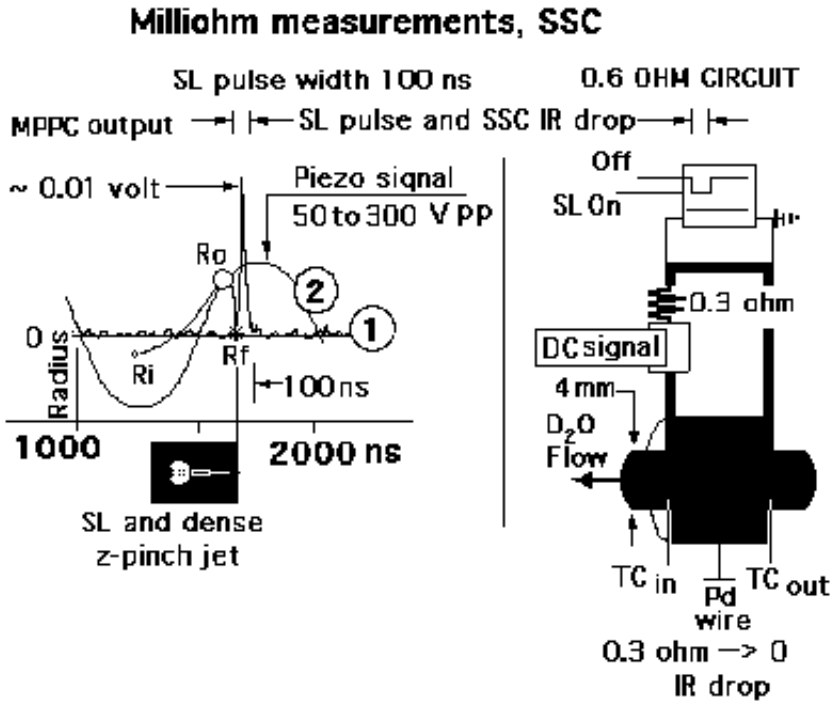

Figure 15. A piezo driven TCB collapse and the measurement of a Pd wire SSC.

One channel measured the acoustic watts input, Ap, at its resonant frequency, and the other the MPPC signal voltage (Fig. 4). The MPPC millivolt signal output generated from an Ap acoustic watt input a sequence of piezo five cycles and shows the resulting coupled sonoluminescence (Fig. 2). The data average of several different Ap values is shown (Fig. 13). The original MPPC signal made up of dark current, other interference, and sonoluminescence photon count was separated into its component parts as the increasing Ap broke its straight line at the MPPC saturation point, $Ap = 2.4$ W, shown in Fig. 13. The break occurs as individual sensing pixels were saturated with photons producing a constant photon count when the 100 pixels of the MPPC are recovering from a photon count, a period of 300 ps. Saturation across the bulk of the MPPC's 1 mm^2 sensing surface area of 100 pixels caused this change of slope in the measured Ap signal.

The photon count was based on the photon saturation point of the MPPC. A number of measurements used the MPPC set at a distance, $d = 8$ cm and $d = 16$ cm (Fig. 4). Varying the Ap watts input from 0.5 to 4.8 W show in Fig. 13 the change in slope reverting to the dark current slope at the MPPC's sonoluminescence saturation point. There were several graphs using different types of MPPC devices and distances that had graphs similar to Fig. 13. The MPPC recovery time was listed as 0.3 ns for all devices. The maximum number of times a pixel could be exposed between saturations, during the 100 ns sonoluminescence pulse duration is 100 ns/0.3 ns = 333 pseudo pixel ratio (Fig. 2). At saturation all pixels are at steady state so the photon count is constant. The MPPC photon counting device sensing area is 0.01 cm^2. The 8 cm distance produces a radiance surface area ratio of 8×10^4. So the total number of photons was about $(8\times10^4)\times(333)\times100 = 2.7\times10^9$ photons at MPPC saturation. The MPPC photon measurements centered at 450 nm with an l spread of 350–900 nm, and therefore did not measure the majority of the UV and VUV photons, but a

relative number of photons; so the actual number may be 10^{10} photons at this 2.4 W Ap saturation setting.

9. Reactor No. 2 Experiment

Superconductivity experiments are ongoing. Ap is used when referring to the acoustics of reactor No. 2 system. Several Hamamatsu MPPC photon detectors that improved photon measurements in reactor 2 devices measured the sonoluminescence. The geometries of the two reactors to accommodate the flow-through calorimetry and piezos were different. The target configurations were different. The general conditions and set-up were the same for both reactors. The temperatures, flow rates, the reactor materials, and argon and D_2O were the same. Jack Forman machined both reactors from polycarbonate blocks. The purpose of these wire experiments was sono-superconductivity, SSC, measurements

The experiment circulated D_2O through a cylindrical 0.3 cm^3 volume at the rate of 2.5 reactor volumes per second of a cylindrical focusing piezo No. 2. The wire was centered and placed in a vertical position, minimizing bubble collection. Piezo measurements involved off and on modes made by the 4 point milliohm meter, to measure any drop in the resistance (Fig. 14). The 17 mm long 100 μm Pd target wire had a resistance 0.332mΩ with electrical contacts using heavy 2 mm diameter copper wire leads of negligible resistance

In the light box, where the wire resistance was measured, red line, no resistance differences were noted (Fig. 14). A varied voltage, 0–120 V, produced a wattmeter input measurement to the oscillator, Q_i, ranging from 0 to 16.4 W and $Ap = 0.3Q_i$ so Ap acoustic input watts varied from 0 to 4.8 W and drove the piezo at its resonance frequency. The red line showed no difference between the piezo off and on mode as the Ap input watts was increased, shown as the blue line. A better measurement technique is shown for sono-superconductivity in Fig. 15. The same basic set-up will use a scope for a quick response to 100 ns looking for an IR that signifies a superconductivity measurement. The 100 μm diameter Pd wire, was part of the measuring circuit and the implantation target, lower right of Fig. 15. The cavitation in D_2O produced an adiabatic collapsing transient cavitation bubble that produced a z-pinch jet and sonoluminescence emission of photons. The implantation process via EM pressure pulse condensed into the dense BEC phase as cluster density maintained a connectivity for 100 ns. The superconducting property depended on the concentration of these sub surface transient BEC elements during the 100 ns period of the sonoluminescence pulse. The left-hand side of Fig. 15 shows the bubble growth, green, and the SL pulse, blue (1), coupling to the piezo acoustic wave resonance, red (2). The right-hand side of Fig. 15 shows the piezo with the flow of circulated D_2O and the low-resistance superconducting measuring circuit, brown, and the oscilloscope measurement of the expected superconducting signal IR drop, red, at every resonance cycle of the piezo. The scope measurement at the top, right box, shows the expected sono-superconducting IR drop, red, during the period of the sonoluminescence. Photon emission measured, 100 ns/acoustic cycle, by the multi pixel photon counter, MPPC.

The sonoluminescence pulse is coupled to 1 MHz resonance of a 17 mm long cylindrical piezo. The 100 μm diameter Pd wire of 0.3 Ω resistance in D_2O, forming the bottom half of the circuit, is in series with 0.3 Ω resistor, black, in a simple circuit powered by a 1 V, DC signal. Any repeating in phase IR drop in the scope total resistance value is a positive response to superconductivity presence. A 1 MHz 100 ns voltage pulse coupled to the piezo resonance frequency can be explained as a BEC steady state concentration level that supports sono-superconductivity and sonofusion. These are ongoing and current experiments

10. Discussion and Summary

The number of transient cavitation bubbles associated with each piezo oscillation, and the geometric differences between reactors Nos. 1 and 2 show that Q_a and Ap, the respective acoustic watt inputs, were different in their bubble distribution and high acoustic bubble densities. Q_a was three times higher in power than Ap. The acoustic watt input, Q_a , of a

cavitating disk piezo at a MHz in D_2O in reactor No. 1, with an energy density, Q_a /m^3, did not change much in a linear piezo acoustic field at small distances, about a millimeter between the disk and the target foil. In reactor No. 2 the acoustic watt input, Ap, of a focused cylindrical piezo acoustic field, with an energy density, Ap/m^3, increased at the wire target surface. Ap/m^3 was inversely proportional to the distance from the active piezo inside surface to the target wire surface (the inside piezo radius). As the Ap acoustic wave moved to the piezo center, the acoustic power density, Ap/m^3, increased. For reactor No. 1 acoustic energy density, Q_a/m^3, at the target foil was proportional to the activity at the Pd foil target surface producing BEC clusters. The sonoluminescence photon and ejecta site counts quantified the transient cavitation bubble's collapse that formed sonoluminescence pulses, z-pinch jets, and BEC cluster formation. The measured ejecta sites support the fact that very small but energetic sources, sub-nanometer in diameter BEC clusters, were produced beneath the target lattice surface. The model shows a correspondence between calorimetric measurements of Q_x, the excess heat and heat of fusion [5], and ejecta sites that can be explained by radiation free DD fusion measured products.

Sonoluminescence pulses and high-density z-pinch jets were produced at the transient cavitation bubble collapse process in the final bubble collapsing radius [9,10]. Some of these z-pinch jets were close enough to implant their high-density deuteron electron plasma into a target. The lattice picosecond implantation and charge separation produced a dynamic EM compression pulse pressure that overwhelmed the Coulombic repulsion escape pressure, and led to a picosecond DD cluster compression fusion environment. The final density of the cluster in this picosecond should have approached 10^{36} deuterons/m^3 for a compressing and cooling environment, promoting DD fusion. The implanting z-pinch jet may form many clusters of various sizes with one fusion event per cluster in the MHz sonofusion devices. Calorimetric measurements were made in reactor No. 1; about 38 W of Q_x were measured (Fig. 5). Here 10^{13} DD fusion events per second produced about 40 W of Q_x from single fusion ejecta sites. A determination by an ejecta site SEM survey could easily support this Q_x measurement. In the MHz reactor No. 2, it was reasonable that the MPPC measurement of 10^{16} photons/s, mostly in UV and VUV range, could also produce the same 40 W Q_x. Sonoluminescence measurements were improved using the MPPC device.

The primary compression pressure was the acceleration of charges to the cluster's center producing an EM pressure pulse surrounded by the electron's magnetic field lines parallel to the cluster surface that cinched down on the shrinking compressing nm cluster, like the nova birth of a white dwarf star. The electron EM pulse formed a cavity enclosing the collapsing deuteron cluster, a pseudo Meissener effect. Except during this picosecond there were moving deuteron charges toward the cluster center. Its strong collapsing magnetic field opposed the direction of the external electron's magnet field. The deuteron's electric field was part of the EM compression pulse also directed to the cluster's center. For a picosecond a dense cluster of D^+ were squeezed together in a BEC (4000 K) with superfluid and superconducting properties (Fig. 6). Energy of fusion in the deuteron BEC was transformed into ^{4}He and heat; Q_x excess heat was produced before the expected 24 MeV gamma mechanism was in place in the BEC environment (gamma production cycle was about 6×10^{-21}/s). In the BEC environment the simplest path for a DD fusion event was to the products of heat, Q_x, and ^{4}He [2]. The deuteron BEC cluster assumed the properties for a picosecond of a high-density liquid for the instantaneous transfer of energy to heat. The ^{4}He and heat products should be favored for this and other implied reasons.

One can add to the cluster's compression by way of the cluster's surface deuteron evaporation that cools the remaining cluster contents via its momentum exchange. The loss of the cluster's surface deuterons cooled the BEC during its compression. The escaping deuterium ion moved into the surrounding Pd target lattice as an ion and its exchange momentum removed heat and added to the compression. After a picosecond, the Coulombic repulsion escape pressures overwhelmed the increasing cluster's compression pulse pressures. In reactor No. 1, sonofusion DD products, deuterons, and vaporized target foil were ejected into the circulating D_2O. Reactor No. 2 produced few fusion products and would be on the path to its BEC superconductor distribution, and denser cluster surface implantation. To strengthen these ideas are theories that predict attractive pressures between dense like charges and Cooper pairs [11],

in a collection of high-density deuterons [12]. These theories might lengthen the picosecond lifetime stability of an implanted positively charged deuteron cluster.

The T_c for a normal ultra cold BEC is a degree or so above absolute zero. The 2.23 MeV, nuclear dissociation energy of the deuteron, fused neutron and proton, could be associated with its unique dissociation of 2.23 MeV. Absence of electrons makes it the lightest elemental boson ion that exists (except [$^1H^{+1}H^+$]). It appears that the deuteron's, D^+, T_c is exceptionally high for its two nucleons, and has the lowest binding energy of any polynuclear nucleus. In the picosecond environment of reactor No. 1 a pair of deuterons fuse. The heat of fusion produced a sub-surface Q_x heat pulse in the cluster that erupts from the target lattice as an ejecta site in the target foil. These sites were observed and surveyed in SEM photos, as evidence of cluster DD fusion and Q_x [2,5]. The clusters' fusion products were ejected along with lattice vapors into the circulating D_2O and then measured. The cluster compression sequence was similar to that of a white dwarf star nova and muon fusion [13]. The cluster was destroyed by the fusion event, a single pair of fusing deuterons in a picosecond EM pulse. The cluster's remnants recombined into D_2O, D_2 and DOOD at steady state concentrations. Reactor Nos. 1 and 2 were density driven systems like muon fusion [14]. If the input acoustic watts, Ap, was adjusted correctly, it allowed for the measured resistance of the transient superconductor using a 4-point milliohm-meter, but the sequence of events was too fast for this measurement system. Because of its transient nature the superconductor resistance could be measured via an oscilloscope keyed to the 100 ns sonoluminescence pulse (Fig. 15).

This model is a good fit for sonofusion's experimental products of ^{4}He and heat of fusion, Q_x, with no gammas. It fits other systems that may have incidental bubbles. The BEC has a possible wider distribution in nature, astrophysically, directed towards dark matter. Several multi-million dollar projects are searching for the axion boson resonance and their connection to dark matter. Under the correct conditions axions will convert to micro-wave photons and back. These will be revealed in the experiments at the University of Washington in the ADMX device. So, some thinking of sonoluminescence pulses and other photon sources and a possible connection to axions is worth consideration [15].

Acknowledgements

I would like to thank the people who saw my DVD presentation at ICCF 16, Robert Zelkovsky who made the ICCF-16 DVD, and Julie Wallace.

References

[1] M.P. Brenner, S. Hilgenfeldt and D. Lohse, Single bubble sonoluminescence, *Rev. Modern Phys.* **74**(2) (2002) 425–484.
[2] R.S. Stringham, *ACS Book, LENR Sourcebook*, J. Marwan and S. Krivit (Eds), Vol. 2, 2009.
[3] R.S. Stringham, *ICCF-14 Proceedings*, D. Nagel and M. Melich (Eds.), Washington DC, USA, 411, Oct. 5–9, 2008.
[4] R.S. Stringham, *ICCF-11 Proceedings*, J.P. Biberian (Ed.), Marseilles, France, Oct.31–Nov. 5, 2004, pp. 238–252.
[5] R. Stringham, *ICCF-10 Proceedings*, P.L. Hagelstein and S.R. Chubb (Eds.), Cambridge, MA, USA, August 24–29, 2003, p. 233.
[6] 17. Brian Oliver; DOE MS analysis of ^{4}He and ^{3}He form EQuest Sciences, report, 1995; Helium Analysis of Gas Samples. B.M. Oliver, Rockwell International, Canoga Park, CA, 91309, 2005.
[7] R. Stringham, *ICCF-8 Proceedings*, F. Scaramuzzi (Ed.), Lerici, LaSpezia, Italy, May 21–26, 2000, pp. 299–304.
[8] R. Stringham, *ICCF-9 Proceedings*, Xing Z, Li (Ed.), *Int. Convention Center*, Tsinghua, Beijing, China, May 19–24, 2002, p. 323.
[9] R.S. Stringham, *JCMNS* **5**(13) (2010), to be published.
[10] Y. Tomita and A. Shima, High speed photographic observations of laser induced cavitation bubbles in water, *Acoustica 71* (1990) 161. P.M. Felix and A.T. Ellis, Laser-induced liquid breakdown – a step by step account, *Appl. Phys. Lett.* **19** (1971) 484. W. Lautterborn and J. Bolle, Experimental investigations of cavitation – bubble collapse in the neighborhood of a solid boundary, *Fluid Mech.* **723** (1975) 91.

[11] E. Muller, Mueller Research Group, Cornell, http://people.ccmr.cornell.edu/ emueller/becbcs.html (2009).
[12] N.L. Lawandy, *Appl. Phys. Lett.* **95** (2009) 234101.

[13] J.D. Jackson, *Phys. Rev.* **106** (1957) 330.
[14] S. Badiei, P. Andersson and L. Holmlid, *Int. J. Hydrogen Energy* **34** (2009) 487–495.
[15] Wikipedia, http://en.wikipedia.org/wiki/Axion (2011).